
Article:
Shafer, J.C., Sulakova, J., Ogden, M.D. orcid.org/0000-0002-1056-5799 et al. (1 more author) (2018) Remediation of potentially acidified Hanford wastes using tri-n-octyl phosphine oxide extraction chromatographic materials. Separation and Purification Technology, 202. pp. 157-164. ISSN 1383-5866

https://doi.org/10.1016/j.seppur.2018.03.029

Highlights:

- A new extraction chromatographic material containing trioctylphosphine oxide is developed for actinide recovery
- The ability of this material to selectively recover actinides potentially acidic Hanford radioactive waste is demonstrated
- The column kinetics are significantly improved when n-dodecane is co-coated with the trioctylphosphine oxide

Remediation of Potentially Acidic Hanford Wastes using Tri-n-octyl Phosphine Oxide Extraction Chromatographic Materials

Jenifer C. Shafer[†], Jana Sulakova[§], Mark D. Ogden[‡], Kenneth L. Nash[*]

Chemistry Department, Washington State University, Pullman, WA USA

ABSTRACT: As the Hanford site undergoes remediation, significant economies could be realized if aluminum and chromium are kept from High Level Waste glass produced at the Hanford Waste Treatment Plant (WTP). An acidic scrub of the Hanford sludge could enhance Al removal, although such treatment could lead to the mobilization of transuranic elements. If mobilization were minor, a chromatographic secondary cleanup of the acidic waste stream may be preferred to allow preconcentration of radionuclides prior to processing through the Hanford WTP. This study examines tri-n-octyl phosphine oxide coated resins as a chromatographic means for the removal of transuranics from a secondary waste stream. Metal uptake kinetics and mechanisms for transuranics and a simulant transuranic (europium) with the developed resin are characterized in both batch and column operation modes. Results indicate up to 99% of the radioactive material present from an acidic sludge leach may be recovered using extraction chromatography providing an effective avenue for high aluminum content tank pre-treatment.

INTRODUCTION

The U.S. Department of Energy (DOE) is responsible for environmental remediation at former nuclear weapons production sites. The Hanford Site, in south central Washington state, was the first facility to produce plutonium for nuclear weapons. Three plutonium separations methods were used during the operation of the Hanford site: Bismuth Phosphate (1945-1956), Redox (1951-1959) and PUREX processes (1956-1972; 1983-1989).[1] The use of multiple plutonium separations and mixing wastes between tanks helped to create a complex waste matrix. As a result, Hanford site remediation is one of the most labyrinthine challenges faced by the Department of Energy. Both the volume and composition of waste resulting from Pu production are major remediation concerns.[2] The most problematic waste component is the sludge created by the caustic environment of the tanks.

The under construction Hanford Tank Waste Treatment and Immobilization Plant (WTP) is the cornerstone of the tank waste remediation effort. Full radioactive operations are scheduled to begin in 2019. The current design of the WTP may not be able treat and immobilize the Hanford tank wastes in the expected lifetime of the plant. Consequently, DOE has been pursuing alternative treatment options for selected wastes. If implemented, alternative treatments could expedite the sludge dissolution process and improve throughput of the WTP, thereby accelerating the overall Hanford tank waste remediation mission.

Remediation treatments efforts have focused on caustic leaching to remove problematic nonradioactive elements aluminum and chromium. Aluminum contributes significantly to the volume of waste processed and the precipitation of chromium spinels from the HLW could short the heating electrodes, clog the pour spout, or otherwise jeopardize the operation and life of the glass melter.[3] Removal of Al and Cr would decrease waste volume, lengthen the lifetimes of the

vitrification furnace and improve stability of the vitrified high level waste (HLW) glass matrix. While not addressed here, the possibility of removing phosphate as an additional pretreatment has also been considred.[4,5] While caustic leaching has proven to have some value, the most stubborn Al phase, boehmite (γ-AlO(OH)), has been resistant to this treatment regimen.

As an alternative, the possibility of using acid/base wash cycles for enhanced alumina removal through surface activation/freshening has been considered. An undesirable side effect of acidic leaching is the potential mobilization of radioactive species into the Al/Cr waste stream.[6] If acidic leaching were to be performed, knowledge of how to remove radioactive species, predominantly actinides, from aqueous media of variable HNO_3 and $Al(NO_3)_3$ concentrations and chromium oxidation states would be required. Previous studies have shown solvent extraction (SX) with 60% by volume (v/v) (TBP) or 0.1 M tri-n-octyl phosphine oxide (TOPO) in *n*-dodecane from nitric acid aqueous media to be a complementary and effective means of handling the secondary cleanup.[7,8] If the solubilization of actinides is low, preconcentration may be desired. An extraction chromatographic remediation could serve to complement the solvent extraction efforts. Extraction chromatographic materials using TBP have also shown to provide reasonable decontamination of transuranics when high concentrations of nitrate are present, but lower concentrations of nitrate require a more basic extractant for recovery of the trivalent actinides.[9]

In this work, a bench scale exploration of a TOPO EXC system for the separation of U, Th, Np, Pu and Eu (serving as a surrogate for the trivalent actinides) from Al/Cr leachate solutions that could emerge if one were to attempt nitric acid leaching with Al-bearing solids has been developed. The “ambient” oxidation state of tracer levels of Np and Pu is defined through comparisons of Np/Pu partitioning with redox stable actinides (Th^{4+} and UO_2^{2+}). The

polyacrylic XAD7 resin was used as the solid support for extractant immobilization as previous studies have shown the XAD7 resin to successfully retain TOPO for the purposes of metal uptake.[10,11] Correlations between solvent extraction chemistry, batch mode extraction and column separations are compared to previous work in this area and with each other.

EXPERIMENTAL SECTION

Materials and Instrumentation

All aqueous solutions were prepared from analytical grade reagents and ultrapure (18 MΩ) deionized H_2O. Solution density was determined by using a calibrated one mL pipette and weighing the aliquot at room temperature. Nitric acid solutions were prepared by mass using Fischer Scientific concentrated (15.8 M) HNO_3 solution. Sodium hydroxide solutions were prepared from dilutions of 50% w/w NaOH (Alfa Aesar) and standardized by titration of potassium hydrogen phthalate to a phenolphthalein end point. Solutions of K_2CrO_4 and $Al(NO_3)_3$ were prepared by mass using analytical grade J.T. Baker solids. The L-ascorbic and 1-hydroxyethane 1,1-diphosphonic acid (HEDPA) solutions were prepared by mass from Fisher Scientific ACS certified reagents and Alfa Aesar, respectively. TOPO (>99%, Sigma Aldrich) was used without further purification and was diluted volumetrically using methanol. Amberlite XAD-7 (Rohm & Hass) was treated as described in the following section.

Experiments using $^{152/154}Eu$, ^{237}Np, $^{233}UO_2$, $^{238}UO_2$,^{238}Pu, and ^{232}Th nitrates were conducted by dilution of standardized stocks from the Washington State University (WSU) radioisotope inventory. Experiments using stable $Eu(NO_3)_3$ were prepared by dilution of standardized stocks. Radioactive $^{152/154}Eu$ was created by neutron activation of 99.999% Eu_2O_3 (Arris International) using a Teaching, Research, Isotopes General Atomics (TRIGA) reactor with a neutron flux of

5×10^{12} n/cm^2·sec at the Nuclear Radiation Center at WSU. Radiotracer experiments using $^{152/154}$Eu were analyzed on a NaI(Tl) solid scintillation counter (Packard Cobra-II auto gamma) for gross gamma counting. Radiotracer experiments using ^{233}U, ^{237}Np and ^{238}Pu were analyzed using a Beckman LS6500 liquid scintillation counter for alpha detection with 5 mL of EcoScint® scintillation fluid. Light metals analysis (Cr, Al) and heavy metal analysis (^{238}U, ^{232}Th) was done using a Perkin Elmer Optima 3200 RL ICP-OES instrument and an Agilent 4500+ ICP-MS, respectively. Mixing was done using a VWR mini vortexer and mass measurements were obtained using a Mettler Toledo XS105 Dual Range series analytical balance.

Resin Preparation

Amberlite XAD7 resin is a polyacrylic resin with a 20-60 mesh particle size and a surface area of 450 m^2/g. Acidic impurities were removed with a DI water rinse until a neutral pH was obtained. Resin drying was expedited by methanol (MeOH) addition and removal, followed by placement in an oven at 80°C for at least an hour. Dried resin was removed from the oven, allowed to cool in a vacuum dessicator, weighed and contacted for 15 minutes by vigorous shaking with 1 M TOPO in MeOH with excess coating solution. Excess solution after contact was removed and the coated resin was dried at 80°C overnight. The amount of extractant loading to the resin is defined in this work as the ratio of mass of organic extractant present to the total final mass of the extractant loaded resin. This coating process provided 58 wt%. For 38 wt% resin, dried resin was contacted in a ratio of 1.05 g XAD7 : 1.75 g TOPO in excess methanol.

The rate of metal uptake onto TOPO-XAD7 resin was determined to be significantly slower than comparable solvent extraction systems. To encourage faster metal uptake kinetics, the TOPO-XAD7 resin was wetted with n-dodecane (abbreviated TOPO-XAD7n) using a 50% v/v chloroform/n-dodecane solution.[12] The 58% and 38% TOPO-XAD7 resins were wetted with 100 and 160 µL of the chloroform/n-dodecane mixture providing dissolution of 30% and 53% of TOPO on the resin surface, respectively. Wetting ratios were selected to minimize the presence of excess n-dodecane and potential loss of TOPO from the resin during the wetting process. Wetting the chromatographic material produced 46% and 24% TOPO-XAD7n resins. Assuming a density of 1 g/mL, which is generally consistent with the literature,[13] the concentration of TOPO for the 46% and 24% wetted resin is 1.33 and 0.75 M, respectively.

Extraction in Batch Experiments

All batch extractions were performed in triplicate and the errors presented denote a ±1σ standard deviation of the triplicate analysis. The weight distribution ratio of the analyte, D_w ($mL \cdot g^{-1}$), was calculated according to the following equation:

$$Dw = \left(\frac{A_o - A_s}{A_s} \right) \times \frac{V}{m} \quad (1)$$

where A_o and A_s are the aqueous phase activity (counts per minute) before and after equilibration, m the mass of resin (g) and V the volume of the aqueous phase (mL). For radiotracer experiments, triplicate experiments showed the reproducibility of the distribution measurements was generally within 10%, although the uncertainty interval was somewhat higher for the highest distribution values ($D_w \geq 10^3$) due to a lack of discernible activity in the aqueous phase. When possible, weight distribution values (D_w) were corrected for nitrate complexation in the aqueous

phase, as done previously, to provide the corrected weight distribution ratio, Dw_o.[7,8] The ratio of solution volume to resin was kept at 10 ml/g.

Eu^{3+} Partitioning

For $^{152/154}$Eu extraction experiments with TOPO-XAD7, the aqueous phase contained various amounts of HNO_3, $Al(NO_3)_3$, Cr(III/VI), and Eu(III). Chromium and ascorbic acid concentrations were maintained at 1 mM and 3 mM, respectively. Europium uptake from varying HNO_3 in the presence of constant $Al(NO_3)_3$ and constant HNO_3 with varying $Al(NO_3)_3$ was studied. Non-radiotracer europium was present at 1 mM to highlight the macroscale uptake capabilities of the TOPO resin. Phases were contacted for 20 minutes by vigorous shaking and aliquots of the aqueous phase were obtained. Analysis for $^{152/154}$Eu in the aqueous phase was performed as described previously.

Actinide Partitioning

Batch investigations were performed for ^{238}U, ^{232}Th, ^{237}Np and $^{152/154}$Eu at tracer concentrations ($<10^{-5}$ M). The concentration of $Al(NO_3)_3$ varied between 0.01 and 1 M while maintaining constant concentrations of HNO_3. Actinide distribution investigations examined a variety of chromium oxidation state conditions and are detailed in the results for a given set of studies. All contacts were for 20 minutes. Aliquots of the aqueous phase were obtained. Analysis for ^{238}U, ^{232}Th and ^{237}Np in the aqueous phase was performed as described above.

Isotherm Determination

Isotherms were generated by monitoring Eu^{3+} or UO_2^{2+} partitioning while increasing the concentrations of Eu^{3+} or UO_2^{2+} from 0.01 mM until the resin was sufficiently saturated. Hypothetical tank conditions of 0.25 M $Al(NO_3)_3$ and 0.1 M HNO_3 were used. Macro concentrations of Eu^{3+} and UO_2^{2+} were provided through the use of stable $^{151/153}Eu$ and longer-lived ^{238}U. These were additionally spiked with $^{152/154}Eu$ or ^{233}U. All contacts were for 30 minutes.

Column Experiments

All column experiments were done with 0.1 M HNO_3 and 0.25 M $Al(NO_3)_3$ to ensure batch mode isotherm results could be directly correlated with column experiments. Some elution volumes are described in terms of *bed volume* (indicating the packed column volume). Columns were Biorad® 1.27 BV PTFE. Columns were weighed before and after column packing with extraction material to provide the mass of the resin used.

The free column volume was determined by extracting a mixed 0.1 M HNO_3/0.25 M $Al(NO_3)_3$ solution into the resin-loaded column. The solution was expelled from the column and weighed. The density of nitric acid/aluminum nitrate solution was determined to be 1.032 ± 0.003. Using the expelled mass and the known density, the free column volume was determined (0.42 ± 0.02 mL). Fractions were collected using a Biorad® 2120 series fraction collector. All aliquots were weighed prior to analysis to quantify fraction size.

Dynamic Capacity Determination

Breakthrough curves were obtained for 58% TOPO/XAD7, 46% TOPO/XAD7n and 24% TOPO/XAD7n systems for Eu^{3+} with initially 1 mM Cr(VI) and 3 mM ascorbic acid present in

solution. Europium concentrations and flow rates may be found in Table 1, which also contains experimental results. The 24% TOPO/XAD7n system had the quickest uptake kinetics and additional breakthrough curves were performed with 1 mM Cr(VI) and 50 mM Eu^{3+} or UO_2^{2+}.

Metal Elution

The elution studies were done under similar conditions used for dynamic capacity determinations. Values from the dynamic capacity determination were used to calculate the Eu^{3+} and UO_2^{2+} stoichiometries under high loading conditions. Flow rates were 50 µL/min for all studies. A 3 BV rinse, 3.81 mL, was done after column loading using a mixed 0.001 M HNO_3/0.75 M $Al(NO_3)_3$ solution. Analyte elution was accomplished as detailed for each experiment. Neptunium and plutonium elution curves had the same load and rinse volumes as the uranium experiments, but only included tracer concentrations of actinides.

RESULTS

Batch Experiment

Metal Partitioning

Figure 1 presents Eu^{3+} distribution data as a function of the total, aqueous nitrate concentration for the TOPO-XAD7 resin. Extraction behavior was determined as a function of increasing $Al(NO_3)_3$ concentration (0.01 M – 1.50 M) at three constant concentrations of HNO_3 (Figure 1a), and also for varied concentrations of HNO_3 (0.01 M – 1.50 M) at two constant concentrations of $Al(NO_3)_3$ (Figure 1b). All distribution data are corrected for complexation of europium by nitrate in the aqueous phase. Corrections for the presence of $Eu(NO_3)^{2+}$ in comparable media have been previously derived.[7,8]

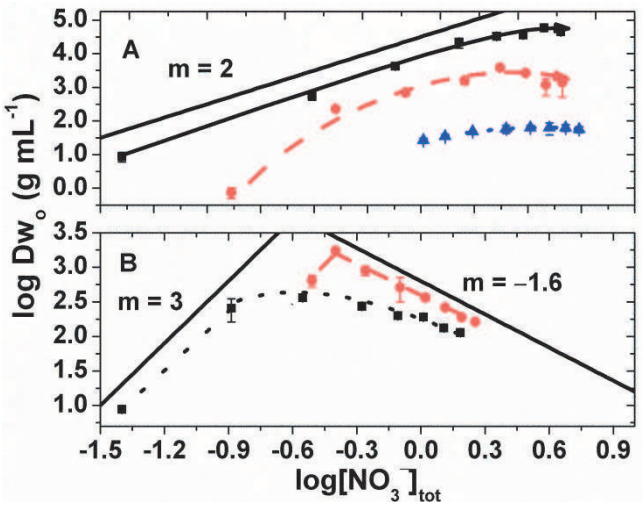

Figure 1. Nitric acid or aluminum nitrate dependences for europium nitrate adsorption into 58% TOPO-XAD7 resin. Lines are provided with slopes (*m*) indicate the dependence of metal extraction on nitrate concentration. Initially present in each aqueous solution was 1.0 mM K_2CrO_4 and 3 mM ascorbic acid. a) Aluminum nitrate varied from 0.01 to 1.5 M, ■ 0.01 M HNO_3 ● 0.10 M HNO_3 ▲1.00 M HNO_3. b) Nitric acid varied from 0.01 to 1.5 M, ■ 0.01 M $Al(NO_3)_3$ ● 0.1 M $Al(NO_3)_3$

The partitioning of Eu^{3+} into the TOPO-XAD7 resins from solutions of constant HNO_3 concentrations increased significantly with increasing concentrations of $Al(NO_3)_3$ (Figure 1a). The highest distribution observed was at $[HNO_3]$ = 0.01 M and $[Al(NO_3)_3]$ = 1.5 M. The partitioning of Eu^{3+} between the TOPO-XAD7 phase from solutions of constant $Al(NO_3)_3$ concentrations with increasing concentrations of HNO_3 (Figure 1b) increased. A maximum in Eu^{3+} recovery was seen at $[HNO_3]$ = 0.25 M and $[Al(NO_3)_3]$ = 0.1 M. A steep decrease, with an approximate slope of -1.6 on the log-log plot, is observed after this maximum.

Figure 2 shows the uptake of Th, U, Np, and Eu at tracer concentrations as a function of $Al(NO_3)_3$ concentration by TOPO-XAD7 resin. The uptake studies of Th^{4+}, UO_2^{2+} and Eu^{3+} served to model the distribution behavior of An^{4+}, AnO_2^{2+}, and An/Ln^{3+} cations, respectively. Comparing uptake behavior between redox active (Np) and redox inactive actinides/lanthanides

(UO_2^{2+}, Th^{4+}, Eu^{3+}) allows an approximation of the anticipated redox state of Np in the sludge simulants for both potentially oxidizing and reducing conditions.

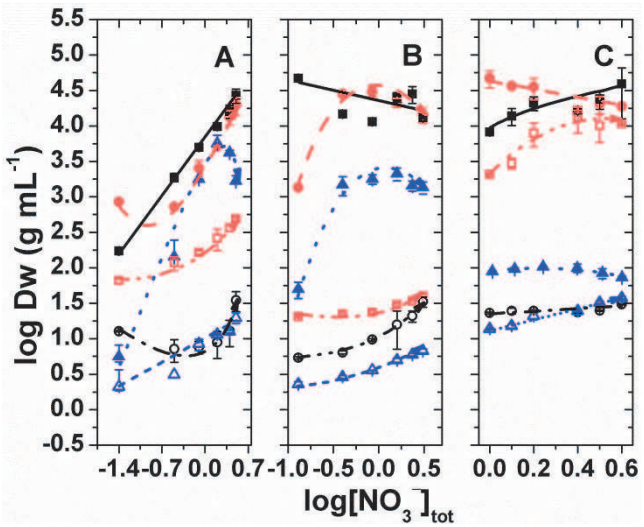

Figure 2. Metal distribution values as a function of aqueous [$Al(NO_3)_3$] with [HNO_3] equal to a) 0.01 M b) 0.1 M and c) 1 M. The various elements and redox conditions described as follows: ■ Th^{4+} ● UO_2^{2+} ▲ Eu ○ Np □ Np, 1 mM CrO_4^{2-} △ Np, 1 mM CrO_4^{2-}, 3 mM ascorbic acid. Solid phase: 100 mg TOPO-XAD7.

Isotherm Determination

Figure 3 compares Eu isotherms of the 58% TOPO-XAD7, 46% TOPO-XAD7n systems and 24% TOPO-XAD7n resins. The data were fit with the ORIGIN® software package using a linear least squares statistical treatment for the Langmuir isotherm model, Equation 2,

$$q_r = \left(\frac{q_{\max} a_L C_e}{1 + a_L C_e} \right) = \left(\frac{K_L C_e}{1 + a_L C_e} \right) \quad (2)$$

where equilibrium concentrations of analyte in the liquid and solid phase, *c* and *q*, respectively, were calculated from Equations 3 and 4;

$$c = \frac{A}{A_o} \cdot c_o \quad (3)$$

$$q = \frac{A_o - A}{A} \cdot \left(\frac{V}{m} \right) \cdot c_o \qquad (4)$$

a_L is the Langmuir constant ($dm^3 \cdot mmol^{-1}$), C_e is the concentration of analyte in the aqueous phase, q_{max} is the maximum mole of analyte sorbed to the resin per gram under static conditions, m is the mass of the resin, V is the volume of aqueous phase, A_o is the initial activity in the aqueous phase (cpm), A is the final activity in the aqueous phase after equilibration, and C_o is the initial concentration of analyte in the aqueous phase, K_L is the Langmuir constant in $dm^3 \cdot g^{-1}$. The calculated saturation stoichiometry of the 24% TOPO-XAD7n resin is 1:3.5 (Eu:TOPO), indicating a mixture of 1:4 and 1:3 complexes in the solid phase.

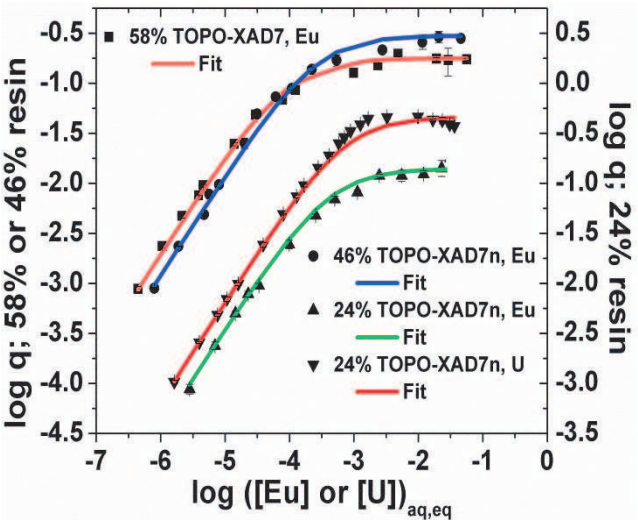

Figure 3. Isotherms comparing the uptake behaviors of europium by the 58% TOPO-XAD7, 46% TOPO-XAD7n and 24% TOPO-XAD7n resin. Uranium isotherm is also shown for the 38% TOPO-XAD7n resin. Initial aqueous phase: 0.1 M HNO_3, 0.25 M $Al(NO_3)_3$, 1 mM K_2CrO_4, 3 mM Ascorbic Acid. Solid phase: 50 mg of the appropriate resin.

Dynamic (Column) Experiments

Practical Dynamic Capacity

Determination of the practical dynamic capacity (*Q(m)*), the maximum number of mmol of analyte per gram of resin under dynamic conditions, was calculated using Equation 5, where *m* is

253 the mass of the solid, c_0 is the initial concentration of analyte, V_o is the free volume of the column
254 and *V(50)* is the volume of solution eluted at 50% breakthrough.

255 $$Q(m) = \frac{V(50) - V_0}{m_s} \cdot c_0 \quad (5)$$

256 Under equilibrium conditions, the determined saturating concentration of analyte in the solid
257 phase should be within error for breakthrough curves (*Q(m)*) and isotherms (q_{max}). Table 1 has a
258 summary of the q_{max} and *Q(m)* values obtained for systems of interest.

259 **Table 1.** Extraction characteristics for various TOPO-XAD7 n-dodecane wetted resins.

	Eu^{3+}			UO_2^{2+}
% TOPO (m/m)	46%	24%	38%	24%
Redox Conditions	1 mM Cr(III)/ 3 mM AA[a]	1mM Cr(III)/ 3 mM AA[a]	1mM Cr(VI)	1mM Cr(VI)
q_{max}*(mmolEu/g resin)*	0.308 ± 0.008	0.176 ± 0.003	-	0.51 ± 0.01
Q(m) (mmolEu/g resin)	0.299 ± 0.009	0.172 ± 0.002	-	0.50 ± 0.02
Flow Rate (µL/mL)	50	50	-	50
D	1200	350	-	640
% recovery	98.3 ± 0.1	99.9 ± 0.3	99.2 ± 0.2	99.7 ± 0.2
Eluent	3 M HNO_3	3 M HNO_3	3 M HNO_3	0.1 M HEDP
Stoichiometry[b]	1:4	1:3.5	-	1:1

260 [a]AA = Ascorbic Acid
261 [b]Is expressed in the ratio metal : ligand
262

263 Figure 4 shows Eu breakthrough curves for all materials examined. Saturating conditions are
264 equivalent (i.e. q_{max} = *Q(m)*; within error) for the 46% TOPO-XAD7n and 24% TOPO-XAD7n
265 isotherms and breakthrough curves. Solvation of TOPO in n-dodecane made the use of higher
266 flow rates possible (up to 50 µL/mL). A higher flow rate (100 µL/min) led to a decrease in the
267 practical dynamic capacity; indicating the system was no longer at equilibrium.

To examine the ultimate remediation capabilities of the 24% TOPO-XAD7n resin for simulated Hanford waste, a simulated waste stream containing 1 mM K_2CrO_4 and tracer

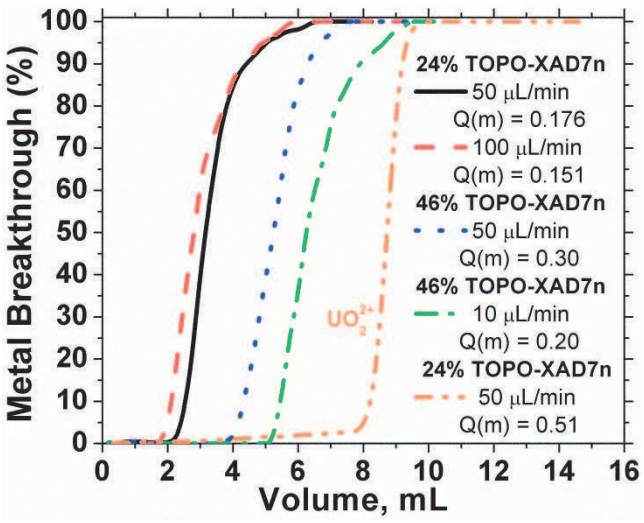

Figure 4. Breakthrough curves comparing the column saturation behaviors of europium by the 46% TOPO-XAD7n and 24% TOPO-XAD7n resin. Uranium behavior is also shown for the 24% TOPO-XAD7n resin. Aqueous Phase: 0.1 M HNO_3, 0.25 M $Al(NO_3)_3$, 1 mM K_2CrO_4, 2 mM Ascorbic Acid. Metal concentration was 50 mM except for breakthrough curve using 46% TOPO-XAD7n resin with a 10 µL/min flow rate, which used 30 mM metal.

$^{152/154}Eu$, ^{233}U, ^{237}Np and ^{238}Pu, simultaneously, was loaded, the resin washed with 0.01 HNO_3 and 0.75 M $Al(NO_3)_3$, and material sequentially eluted with 3 M HNO_3 and 1 mM $KBrO_3$ to recover Eu, then 0.1 M HEDPA and 1 mM $KBrO_3$ to recover the actinides. The addition of potassium bromate ensured oxidation of Np and Pu to their hexavalent states in the absence of chromate. Figure 5 shows the semi-logarithmic elution curves obtained for the simulated waste experiment.

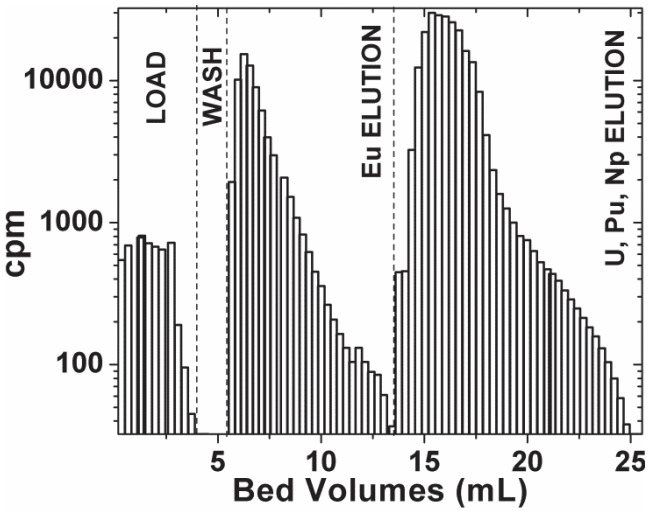

Figure 5. Loading and elution of U, Pu, Np and Eu by 24% TOPO-XAD7n column from simulated waste stream containing 1mM K_2CrO_4, 0.1 M HNO_3 and 0.25 M $Al(NO_3)_3$ shown on a semi-log scale to allow viewing of column tailing. Elution of Eu was performed using 3 M HNO_3 and 1 mM $KBrO_3$ to retain Np and Pu in the hexavalent state in the absence of chromate. Elution of actinides was performed using 0.1 M Etidronic Acid (HEPA) and 1 mM $KBrO_3$.

DISCUSSION

Europium Partitioning

The availability of $^{152/154}$Eu and its comparable uptake behavior to the lanthanides and the trivalent actinides for solvating organophosphorus extractants made this isotope an ideal candidate to screen potential TOPO-XAD7 supports. For $^{152/154}$Eu investigations, the aqueous phase conditions were similar to previous solvent extraction investigations.[5,6,11] These conditions have been selected to represent a wide range of possible solutions that could be encountered during tank sludge leaching with HNO_3 solutions. For discussion purposes, *oxidizing conditions* or *reducing conditions* are defined as the inclusion of 1 mM K_2CrO_4 or 1 mM K_2CrO_4/3 mM ascorbic acid in the aqueous phase, respectively.

Europium extraction by the TOPO-XAD7 resin increased as the concentration of $Al(NO_3)_3$ increased (Figure 1a). The negative slope observed on the logarithmic plot of Figure 1b at

higher nitrate concentrations could be generated by an ion exchange mechanism for Eu^{3+} uptake. The conventional extraction mechanism and proposed ion-exchange mechanisms are shown as Equations 6 and 7, respectively, where n = 3 or 4 and X ≤ 2. Cation exchange uptake mechanisms by solvating extractants have been proposed previously in the presence of highly acidic media.[14]

$$Eu(NO_3)_x^{3-x} + TOPO(HNO_3)_{3-x} \rightarrow Eu(TOPO)(NO_3)_3 + (3-x)H^+ \quad (6)$$

$$Eu(NO_3)_x^{3-x} + \overline{nTOPO(HNO_3)_{3-x}} \rightarrow \overline{Eu(TOPO)_n(NO_3)_3} + (3-x)H^+ \quad (7)$$

Verification of this using slope analysis would require solution activity to be accounted for in the mixed electrolyte solution. In agreement with previous liquid-liquid extraction studies, results here indicate higher concentrations of $Al(NO_3)_3$ would be preferential to encourage decontamination of low level leachates. Extraction increases in the presence of aluminum nitrate can be related to the decline in water activity allowing more effective release of the Eu^{3+} to the organic phase (i.e. salting out).

Actinide Partitioning with TOPO-XAD7

Expectedly, the presence of $Al(NO_3)_3$ had a similar "salting out" effect for both actinide and lanthanide uptake. Modeling of the system with UO_2^{2+}, Th^{4+}, and Eu^{3+} shows the extraction preference for the TOPO-XAD7 system is $An^{4+} > AnO_2^{2+} > An^{3+} > AnO_2^{+}$. This trend can be directly related to the effective charge, Z_{eff}, which is 4, 3.3, 3, and 2.2 for An^{4+}, AnO_2^{2+}, An^{3+}, and AnO_2^{+}, respectively.[15] The extraction trend demonstrates that electrostatic interactions dominate chemical interactions of the f-elements with the organophosphorus reagent. Based on the uptake results of Th^{4+}, Np^{4+} does not appear to be significantly present in any of the potential waste conditions. Plutonium is expected to be in the trivalent state[16] in solutions containing

ascorbic acid and in the hexavalent state for oxidizing conditions.[17] The redox speciation of Np in high ionic strength media and dilute nitric acid is relatively unknown. An additional complication is that chromate and neptunium can be reduced and oxidized, respectively, by trace nitrate impurities.[18-20]

Neptunium Chemistry

Neptunium redox chemistry produced more nuanced uptake patterns for neptunium in contrast to the other redox stable f-elements. Redox potentials in Table 2 indicate that the reducing capability of ascorbic acid for Np decreases with decreasing pH.[21] Chromate is also more readily reduced to chromium (III) at lower pHs. Pourbaix predominance diagrams note that hexavalent neptunium will reduce to the pentavalent state in aqueous media when acidic concentrations are below 0.01 M due to water stability issues and that both tetravalent and hexavalent oxidation states are stable under higher acid conditions.[24] These parameters frame an explanation for neptunium redox speciation and subsequent uptake by the TOPO-XAD7 resin. Later studies could additionally consider the redox speciation of plutonium, which generally has richer redox chemistry than neptunium.

At low acid concentrations (0.01M), neptunium distribution is comparable for systems without chromium and with reduced chromium (courtesy ascorbic acid) – indicating that NpO_2^+ is the predominant neptunium species present in solution. Neptunium in contact with chromate is at least partially oxidized, as indicated by better extraction, but uptake is not comparable to UO_2^{2+}, the stable hexavalent actinide model. This is probably related to water stability issues identified on the Pourbaix predominance diagram limiting Np oxidation and extraction.

Table 2. Neptunium redox reaction significant to understanding simulated acidic aqueous raffinate of the Hanford tanks.[19,20,22]

Reaction	E^o(V)
$NpO_2^+ + 4H^+ + e^- \rightarrow Np^{4+} + 2H_2O$	0.567
$NpO_2^{2+} + e^- \rightarrow NpO_2^+$	1.236
$NO_3^- + 3H^+ + 2e^- \rightarrow HNO_2 + H_2O$	0.94
$NpO_2^{2+} + HNO_2 + H_2O \rightarrow NpO_2^+ + NO_3^- + 3H^+$	0.296
$\text{Dehydroascorbic Acid} + 2H^+ + 2e^- \rightarrow \text{Ascorbic Acid}$	0.390
$HCrO_4^- + 7H^+ + 3e^- \rightarrow Cr^{3+} + 4H_2O$	1.20

At mid-level acid concentrations (0.1 M), Np extraction is more comparable between the various conditions examined. Under oxidizing conditions, chromate reduction at higher acid concentrations prevents significant oxidation of Np, but there still appears to be slightly more Np(VI) than in other 0.1 M HNO_3 studies. Hexavalent neptunium would also provide increased uptake, but, considering the reducing conditions of the system, this is unlikely. Neptunium uptake for the system lacking chromium is low – indicating that pentavalent neptunium as predominant. At the highest acid concentrations studied (1 M), neptunium extraction is nearly identical for the no chromium and the chromium/ascorbic acid containing systems. For the chromate containing system, neptunium TOPO-XAD7 uptake comparable to uranium is observed. Neptunium in this instance appears predominantly in the hexavalent state.

Considering the variability of redox factors, if acidic recovery of the Hanford tanks were attempted, further studies would be necessary to evaluate the redox speciation of the relevant redox active actinides (Np and Pu) to develop effective low-level recovery processes. If a secondary cleanup is required of the Hanford sludges (and conditions are not oxidizing), a

364 balance between sufficient nitric acid for oxidation of Np while preventing competition between
365 with nitric acid for the TOPO available in the system would be required.
366
367 **Static and Dynamic Capacity Determination**
368 Isotherms and breakthrough curves allow determination of resin saturation for batch (static)
369 and column (dynamic) modes, respectively. Examining column behavior at heavy metal loading
370 will show if the column maintains reasonable performance at higher load concentrations. If
371 analyte uptake is reaching equilibrium, the resin should behave comparably regardless of the
372 mode of operation. Comparable behavior allows validation of the values obtained for analyte
373 uptake. A summary of parameters determined for both static and dynamic mode behavior is
374 shown in Table 1. Overall, the 38% TOPO-XAD7n resin showed the excellent reproducibility
375 between static and dynamic modes.
376
377 *Static Extraction Capacity Determinations*
378 Several assumptions are required for the Langmuir model to be valid: the surface of the
379 adsorption must be uniform, the adsorbed molecules must not interact, all adsorption must occur
380 through the same mechanism, and at maximum sorption only a monolayer can be formed.[25]
381 Figure 3 shows the Langmuir fit of the saturation isotherm generally describes europium and
382 uranium uptake and analyte concentrations that provide a saturated resin. Saturation conditions
383 were observed for all 58% TOPO-XAD7 resins at 30 mM Eu. For 24% TOPO-XAD7n resin, the
384 saturating concentrations for Eu^{3+} and UO_2^{2+} were greater than 25 mM of metal. To ensure
385 saturation, breakthrough experiments later were performed with at least 30 mM Eu^{3+} or UO_2^{2+}.

Saturating stoichiometries (Eu:TOPO) of 1:5 and 1:4 are calculated for the 58% TOPO-XAD7 and 46% TOPO-XAD7n resins, respectively. This indicates a more efficient usage of the n-dodecane wetted material. Typical stoichiometries in solvent extraction systems have noted 1:3 Eu:TOPO extracted species[26]; however, since the concentration of TOPO on the resin (>1 M) is an order of magnitude greater than typically used in solvent extraction systems, this excess of TOPO could lead to a larger number of extractant molecules binding with Eu. Nitrates can be bound to a metal ion in a monodentate or bidentate fashion. Assuming the coordination of three bidentate nitrate ions, this would produce a coordination number of 10 for the extracted metal ion. Coordination numbers of 8-9 are typically observed with lanthanides in a solution matrix. Crystal structures have shown lanthanides to have coordination numbers as high as 12 in the solid state. Since the extraction chromatographic system represents a hybrid between the solution phase and a crystalline phase, a higher coordination number may not be unreasonable.

The information obtained through initial europium experiments narrowed uranium saturation investigations to only the 38% TOPO-XAD7n resin. Stoichiometries for Eu^{3+} and UO_2^{2+} in contact with the 38% TOPO-XAD7n resin were 1:3.5 for Eu:TOPO and 1:1 for UO_2:TOPO complexes, respectively. The additional dissolution of TOPO appears to have aided in creating an environment similar to the solvent extraction system. The 1:1 stoichiometry of the UO_2^{2+}:TOPO complex was unanticipated. Typically a 1:2 stoichiometry is observed between uranium and TOPO in solvent extraction systems.[27]

Dynamic Extraction Capacity Determination

Figure 4 shows the breakthrough curves obtained for the TOPO-XAD7n resin with Eu^{3+} and UO_2^{2+}. As noted in the previous section, initial europium screening showed analyte uptake

kinetics of the 24% TOPO-XAD7n where favorable compared to the 36% TOPO-XAD7n. Uranium uptake was studied exclusively with the 38% TOPO-XAD7n resin. Given the unique data obtained regarding Eu:TOPO stoichiometries, the practical dynamic capacity, *Q(m)*, obtained from the breakthrough curves was particularly useful in validating the saturating values for Eu^{3+} for each of the n-dodecane wetted materials examined thus far. Table 1 notes the agreement between *Q(m)* and q_{max} for the n-dodecane wetted materials.

Simulated Waste Stream Remediation

The simulated waste stream contained 0.1 M HNO_3, 0.25 M $Al(NO_3)_3$, 1 mM K_2CrO_4, 30 mM Eu and U, and tracer Pu and Np. Oxidizing conditions were highlighted in this experiment to examine loading effects that could occur if hexavalent, extractable actinide species were present. The 0.1 % breakthrough observed during the loading step in the single, Pu, Np and U experiments (not shown) and the lack of breakthrough during the wash step was also observed with the simulated waste stream. No evidence of Eu breakthrough during the load step was observed using either gamma or liquid scintillation spectroscopy. Europium elution occurred without any detectable evidence for alpha activity (indicative of actinide recovery) observed using liquid scintillation detection. The elution of Eu was quantitative within error. Removal of the actinides was comparable to the single element experiments. The higher actinide loading for the simulated waste stream increased the column tailing, observed in the semi-log curve (Figure 6); however, recovery was within error still quantitative. A smaller mesh size resin would most likely improve the column stripping kinetics and reduce tailing.

Although the decontamination of the simulated Al leachate waste stream using extraction chromatography is comparable to the decontamination obtained in solvent extraction

investigations, throughput and column blockage can be drawbacks to the implementation of chromatography on a large scale. Extractant loss occurs in both liquid-liquid and extraction chromatographic methods. If the extractant were covalently bound to a polymer (instead of merely held in place by solubility preferences), chromatographic separations of nuclear fuel may become preferential. Several such resins are currently in development.[28,29]

AUTHOR INFORMATION

Corresponding Author

*knash@wsu.edu; (509) 335-2654 (K.L.N.)

Present Addresses

[†]Department of Chemistry, Colorado School of Mines, Golden, CO USA

[‡]Department of Chemical and Biological Engineering, University of Sheffield, United Kingdom

[§]Czech Technical University, Radiochemistry Department, Prague, Czech

ACKNOWLEDGMENT

The authors would like to thank the Department of Energy Environmental Management Science Program for funding this work. An acknowledgement is due to the Nuclear Radiation Center (NRC) at WSU for the production of the Eu radioisotopes used in this study.

455

456 REFERENCES

457 1. Agnew, S.F. Hanford Defined Wastes: Chemical and Radionuclide Compositions. *LAUR-94-*
458 *2657Rev 2*, Los Alamos National Laboratory, Los Alamos, New Mexico.

459 2. DeMuth, S.F.; Thayer, G.R. An Updated Cost Study for Enhanced Sludge Washing of
460 Radioactive Waste. *Remediation Journal*, **2002**, 87 – 97.

461 3. Vienna, J.D.; Hrma, P.; Crum, J.V.; Mika, M. Liquidus temperature-composition model for
462 multi-component glasses in the Fe, Cr, Ni, and Mn spinel primary phase field. *J. Non-cryst. Sol.*
463 **2001**, *292* (1-3), 1-24.

464 4. Lumetta, G.J; Braley, J.B.; Peterson, J.M.; Bryan, S.A.; Levitskaia, T.G.; Separating and
465 Stabilizing Phosphate from High-Level Radioactive Waste: Process Development and
466 Spectroscopic Monitoring. *Environ. Sci. Tech.* **2012**, *46* (11), 6190−6197.

467 5. Lumetta, G. J.; Felmy, A. R.; Braley, J. C.; Carter, J. C.; Edwards, M. K.; MacFarlan, P. J.;
468 Qafoku, O. *Removing Phosphate from Hanford High-Phosphate Tank Wastes: FY 2010 Result*s;
469 PNNL-19778; Pacific Northwest National Laboratory: Richland, WA, **2010**.

470 6. Bond, A.H.; Nash, K.L.; Gelis, A.V.; Sullivan, J.C.; Jensen, M.P.; Rao, L. Plutonium
471 mobilization and matrix dissolution during experimental sludge washing of bismuth phosphate,
472 Redox, and PUREX waste simulants. *Sep. Sci. Tech.* **2001**, *36* (5&6), 1241-1256.

473 7. Harrington, R.C. Separation of Hanford Tank Wastes by Liquid-Liquid Extraction Employing
474 Organophosphorus Extractants. M.S. Thesis, Washington State University: Pullman, **2006**.

475 8. Harrington, R.C.; Martin, L.; Nash, K.L.; Partitioning of U(VI) and Eu(III) between acidic
476 $Al(NO_3)_3$ and tributyl phosphate in n-dodecane. *Sep. Sci. Tech.* **2006**, *41* (10), 2283-2298.

477 9. Braley, J.C. The use of organophosphorus extractants in f-element separations.Ph.D Thesis,
478 Washington State University: Pullman, **2010**.

479 10. Yamaura, M.; Matsuda, H.T. Actinides and fission products extraction behavior in
480 TBP/XAD7 chromatographic column. *J. Rad. Nucl. Chem.* **1997**, *224* (1-2), 83-87.

481 11. Navarro, R.; Gallardo, V.; Saucedo, I.; Guibal, E. Extraction of Fe(III) from hydrochloric
482 acid solutions using Amberlite XAD-7 resin impregnated with trioctylphosphine oxide (Cyanex
483 921). *Hydrometallurgy* **2009**, *98* (3-4), 257-266.

484 12. Sulakova, J. Study of solid extractants for separation of minor actinides from high active
485 liquid waste, Ph.D. Thesis, Czech Technical University: Prague, 179, **2007**.

486 13. Braun, T.; Ghersine, G. *Extraction Chromatography*. Elsevier Scientific Publishing Co.: New
487 York, NY, **1975**.

488 14. Alexandratos, S.D.; Zhu, X. Bifunctional coordinating polymers: Auxiliary groups as a
489 means of tuning the ionic affinity of immobilized phosphate ligands. *Macromolecules* **2005**, *38*
490 (14), 5981-5986.

491 15. Choppin, G.R.; Rao, L.F. Complexation of pentavalent and hexavalent actinides by fluoride.
492 *Radiochimica Acta* **1984**, *37* (3), 143-146.

493 16. Poczvnajlo, A.; Janiszewski, Z.; Al-Shukrawi, H. The use of ascorbic acid for reductive
494 separations of plutonium from uranium. *Nukleonika*. **1988**, *33* (7-9), 203-218.

17. Weigel, F.; Katz, J.J.; Seaborg, G.T. in *The Chemistry of the Actinide Elements, Second Edition, Vol. 1,* J.J. Katz, G.T. Seaborg and L.R. Morss, Eds. Chapman and Hall: London, U.K. **1986**, p. 499.

18. Escure, H.; Gourisse, D.; Lucas, J. Dismutation du neptunium pentavalent en solution nitrique—I: Etudes a l'equilibre. *J. Inorg. Nucl. Chem.* **1971**, *33* (6), 1871-1876.

19. Ananiev, A.V.; Shilov, V.P.; Moisy, Ph.; Madic, C. Heterogenous catalytic oxidation of neptunium (IV) in nitric acid solutions. *Radiochimica Acta* **2003**, *91* (9), 499-503.

20. Hsu, C-L.; Wang, S-L.; Tzou, Y-M. Photocatalytic presence of NO_3^- and Cl^- electrolytes as influenced by Fe(III). *Env. Sci. Tech.* **2007**, *41* (22), 7907-7914.

21. Ruiz, J.J.; Aldaz, A.; Dominguez, M. Mechanism of L-ascorbic acid oxidation and dehydro-L-ascorbic acid reduction on a mercury electrode. I. Acid medium. *Can. J. Chem.* **1977**, *55* (15), 2799-2806.

22. Tochiyama, O.; Nakamura, Y.; Hirota, M.; Inoue, Y. Kinetics of nitrous acid-catalyzed oxidation of neptunium in nitric acid-TBP extraction system. J. Nucl. Sci. Tech. **1995**, *32* (2), 118-124.

23. Burney, G.A.; Harbour, R.M. Radiochemistry of Neptunium. **1974**, *NAS-NS-3060* US Atomic Energy Commission.

24. Pourbaix, M.J.N. *Atlas of Electrochemical Equilibriums in Aqueous Solutions*, 2nd ed.; Natl. Assoc. Corrosion Engs.: Houston, TX, 1974.

25. Strumm, W. *Chemistry of the Solid Water Interface: Processes at the Mineral Water and Particle Water Interface in Natural Systems*. John Wiley & Sons, Inc.: New York, NY, **1992**.

26. Foffart, J.; Duyckaerts, G. Extraction of lanthanides and actinides by alkylphosphine oxides. IV. Extraction of trivalent cations by tri-n-butylphosphine oxide or tri-n-octyl phosphine oxide. *Analyt. Chim. Acta* **1969**, *46* (1), 91-9.

27. Watanabe, K. Extraction of thorium and uranium from chloride solutions by tributyl phosphate and tri-n-octylphosphine oxide. *J. Nuc. Sci. Tech*. **1964**, *1* (5), 155-62.

28. Alexandratos, S.D.; Zhu, X. High-affinity ion-complexing polymer-supported reagent: Immobilized phosphate ligands and their affinity for the uranyl ion. *React. Polym*. **2007**, *67* (5), 375-382.

29. Alexandratos, S.; Xiaoping, Z. Immobilized phosphate ligands with enhanced ion affinity through supported ligand synergistic interaction. *Sep. Sci. & Tech*. **2008**, *43* (6), 1296-1309.